Raypath interferometry for dummies

David C. Henley

ABSTRACT

We illustrate here the key processing steps used to apply raypath interferometry to the source or receiver gathers of a 2D seismic line in order to remove the time/phase disturbances due to the near-surface of the earth. While we don't show all the processing steps, we show the important ones. We illustrate the processing flows with examples from two different sets of field data.

RAYPATH INTERFEROMETRY BY THE NUMBERS

We show ***7 basic steps*** in the application of raypath interferometry:

1. Transform input gathers to the radial trace ***(R-T) domain***—(Figures 1 and 2)

2. Sort R-T traces to common-angle gathers—(Figures 3 and 4)

3. Create pilot trace gathers using horizon picks—(Figures 5, 6, 7, and 8)

4. Correlate pilot trace and raw trace common-angle gathers—(Figures 9 and10)

5. Apply inverse filters to raw common-angle gathers—(Figures 11 and 12)

6. Re-sort corrected common-angle gathers to ***R-T transforms***—(not illustrated)

7. Inverse transform R-T gathers to ***X-T domain***—(not illustrated)

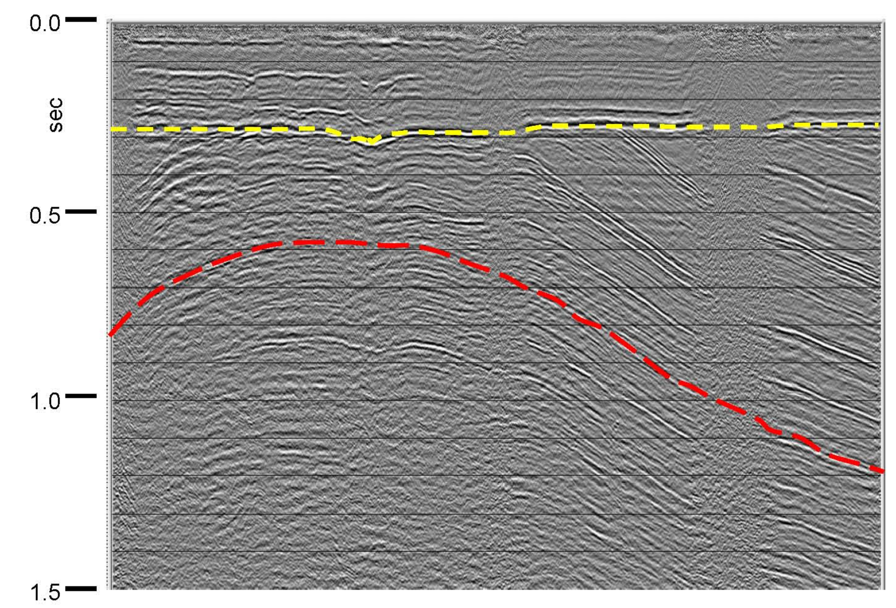

Brute stack shown with shallow and deep pilot trace horizons

FIG. 5. A brute stack from the MacKenzie Delta, showing two horizons picked for pilot trace building purposes. The horizons are the 'smoothing directions' used to make pilot traces.

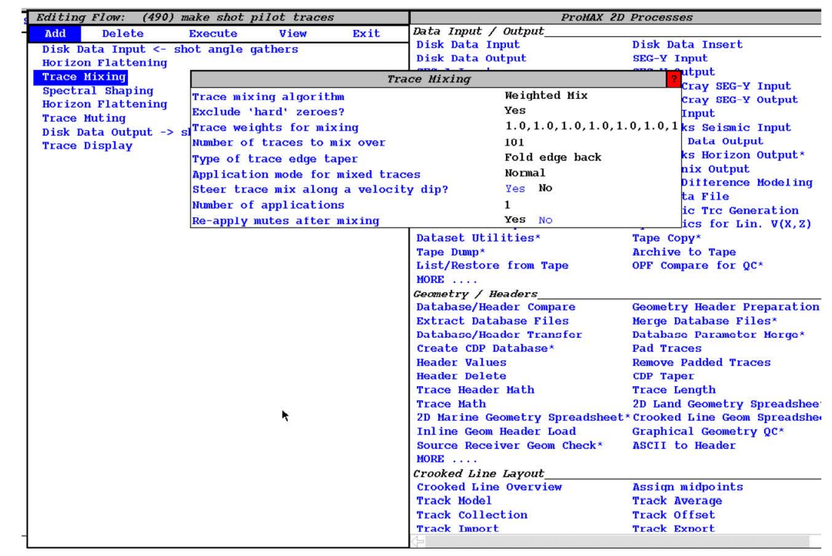

Flow for creating pilot traces for one picked horizon from constant-angle gathers. First horizon flattening applies horizon times, second removes them after trace mixing. Spectral shaping whitens pilot traces, trace muting zeros portions of pilot traces which do NOT conform to the picked horizon. This flow is applied once for each horizon picked on the brute stack to create sets of horizon pilot traces.

FIG. 6. This processing flow shows one way to create pilot traces by smoothing along a picked horizon. The flow can be used for each of several horizons to create windows of pilot trace segments that can be subsequently merged, as in Figure 8.

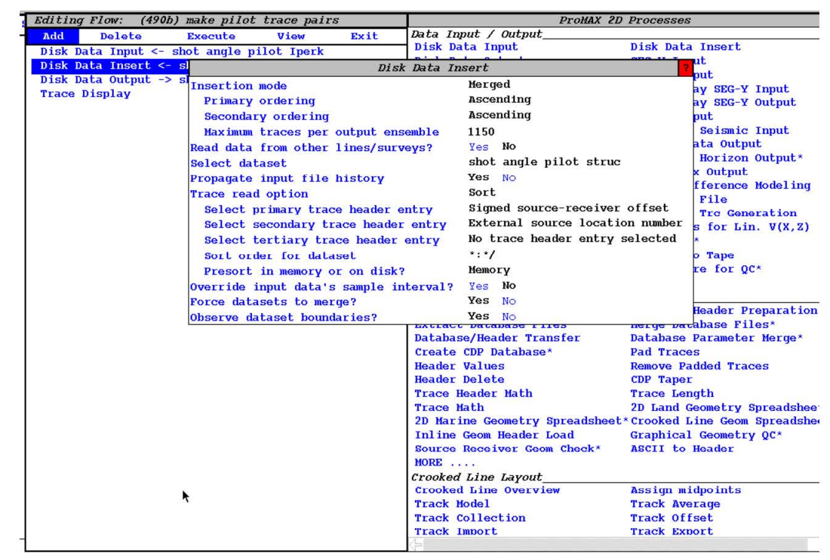

Flow to merge two sets of horizon pilot traces. The disk data insert adds a new set of horizon pilot traces, so that the output is a set of constant-angle gathers with two horizon pilot traces at every shot position. These traces will be summed in the subsequent flow to make composite pilot traces.

FIG. 7. This flow shows how to merge two sets of horizon-smoothed pilot traces. A subsequent flow would sum the trace pairs into a pilot trace panel like that shown in Figure 8.

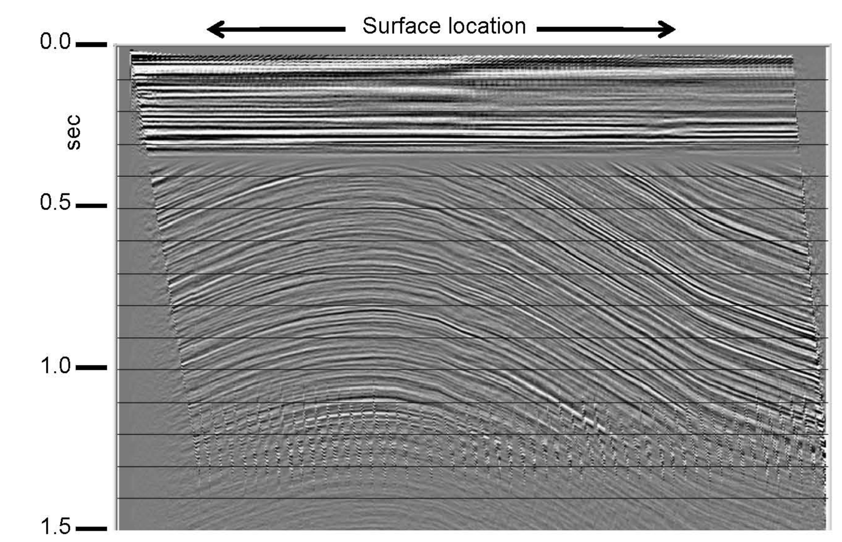

FIG. 8. This an example of a pilot trace common-angle gather created for the raypath angle of -231 m/s for the MacKenzie Delta survey.

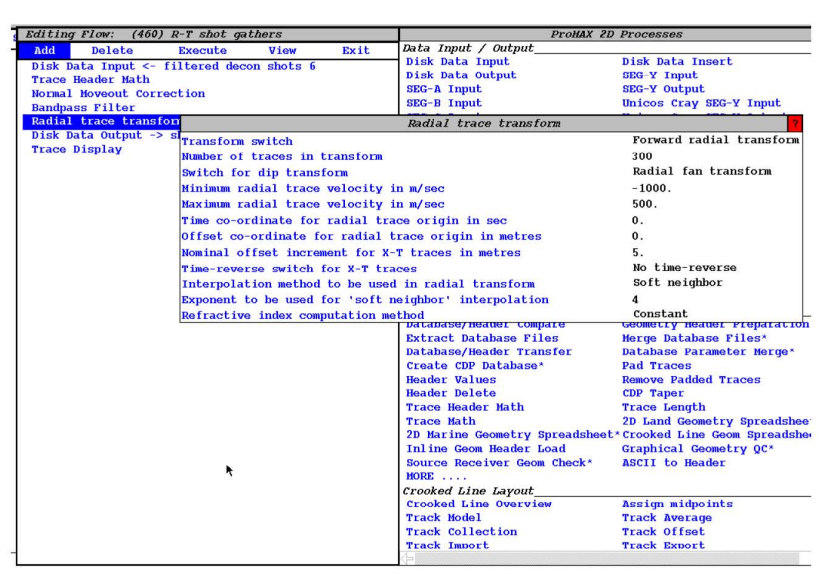

Flow for reading shot gathers and transforming to the radial trace domain. Parameters in the transform are data-dependent. Minimum and maximum velocities should define a fan which captures most of the gather…number of traces should be at least 300-500 to avoid aliasing sh gather. Normal moveout correction need only use an approximate function

FIG. 1. This processing flow transforms a source (receiver) gather to the radial trace (R-T) domain, where raypath angles are constant for each trace.

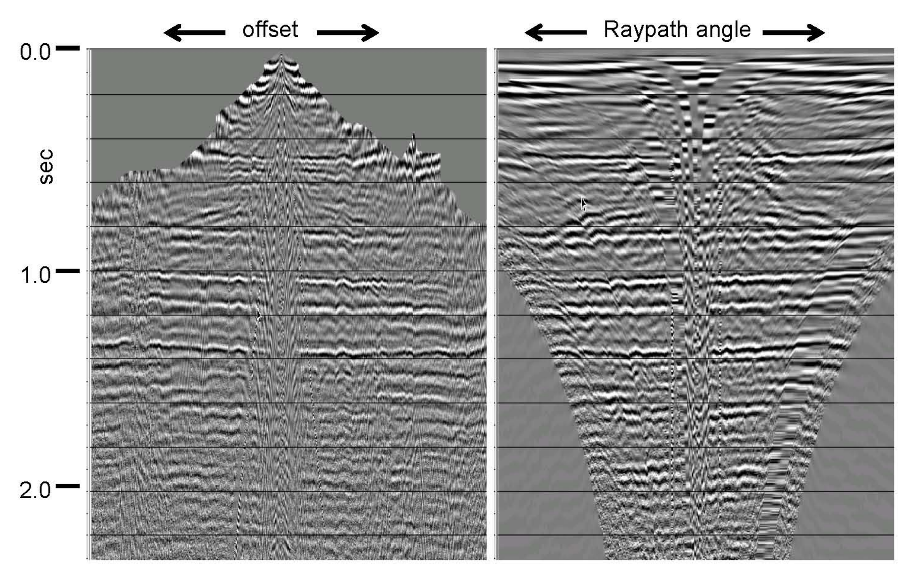

FIG. 2. An NMO-corrected shot gather from the Spring Coulee vertical component data set (left) transformed to the radial trace (R-T) domain (right). Note that reflections don't change much in appearance from one domain to the other

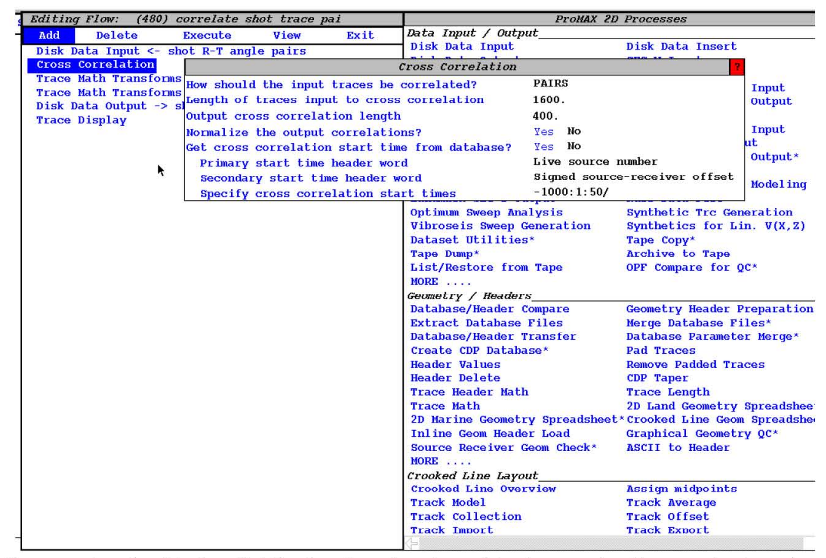

This flow creates the 'statics distribution functions' used to deconvolve the constant-angle traces. The correlations use basically the entire input trace and its matching composite pilot trace, and the output correlation length is long enough to include any conceivable 'static'. The first trace math transform raises each sample to an odd power (often 5) to whiten the function without adding new peaks, while the second applies a Hanning window.

FIG. 9. After the pilot traces (Figure 8) and their corresponding raw traces are merged (in a step similar to that shown in Figure 7), the cross-correlation and 'conditioning' steps are carried out in the flow shown here

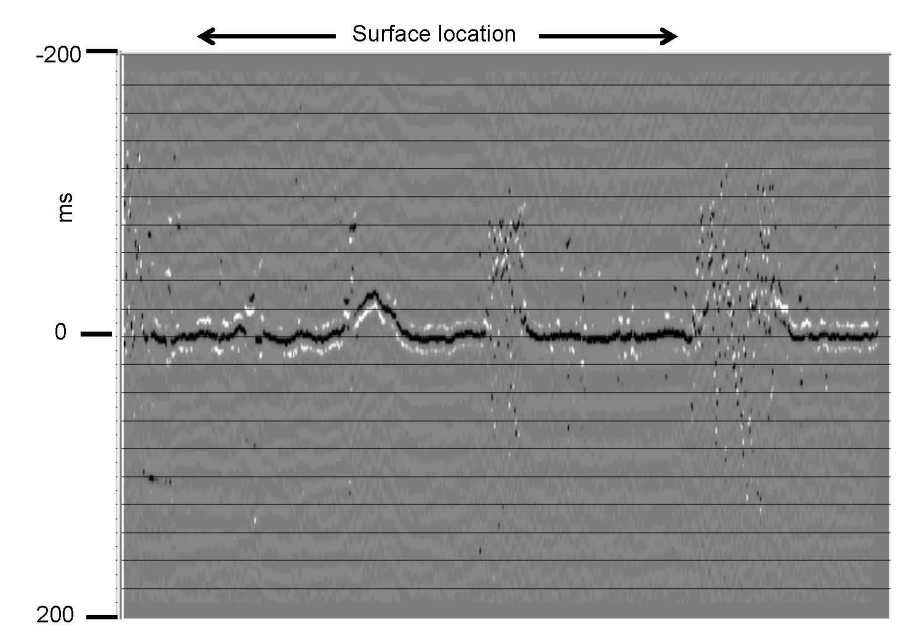

FIG. 10. An example of some 'conditioned' cross-correlation functions created by the flow in Figure 9. A panel of such functions is created for each common-angle gather in the data set. Inverse filters are derived directly from these 'statics' functions.

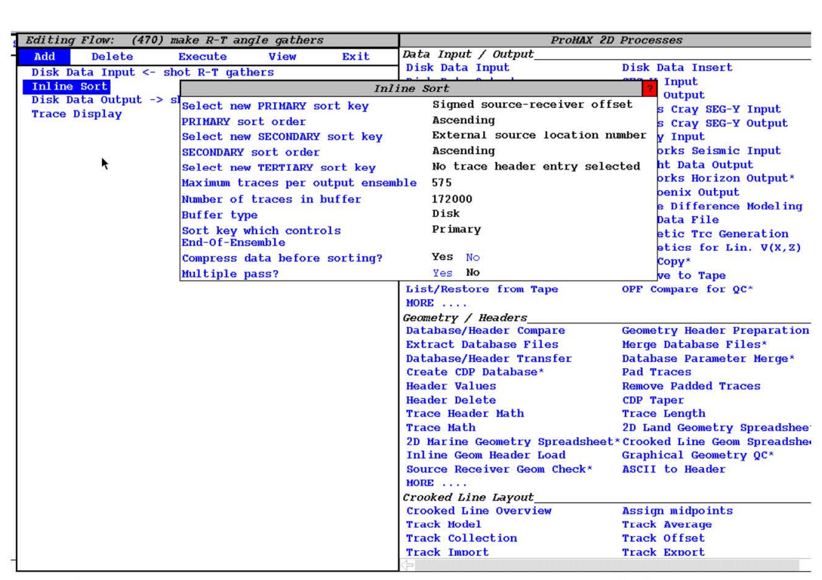

Flow for sorting radial trace gathers into 'constant-angle gathers'. The 'offset' header of each radial trace contains the apparent velocity used to gather the samples for that trace from the original X-T shot gather; so sorting by signed offset, then external source location creates a 'constant-angle gather' for each apparent velocity value.

FIG. 3. This processing flow sorts the radial traces by raypath angle (apparent velocity) and surface location to create 'common-angle' gathers.

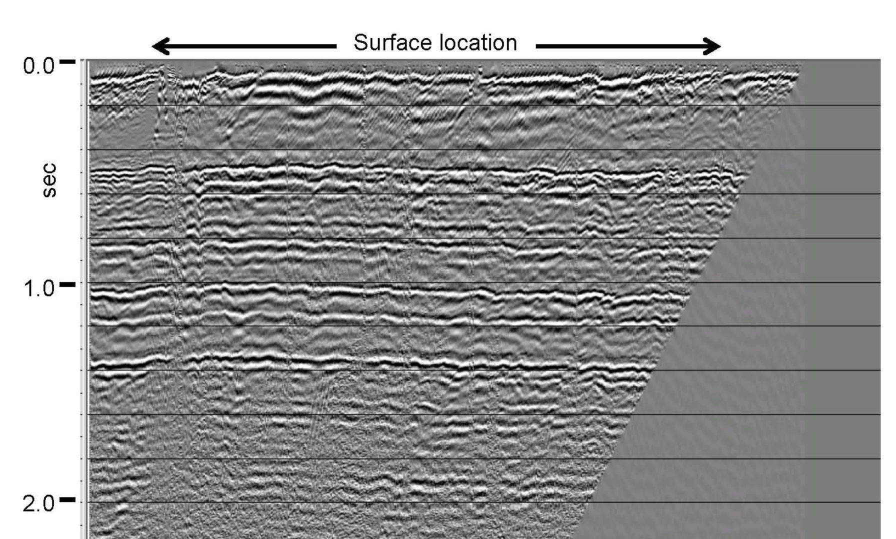

Common angle gather for vertical component receiver data for angle of -898 m/s. Arrow marks event to match with inline data

FIG. 4. An example of a common-angle gather for the Spring Coulee vertical component data set. Several hundred common-angle gathers are created, depending upon the parameters chosen in the radial trace transform.

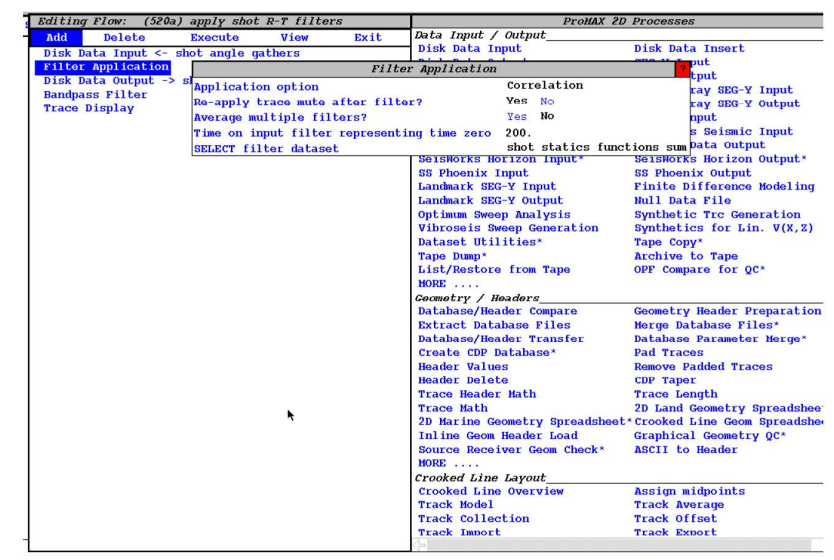

This flow applies the match filters or inverse filters to the constant-angle gathers, trace-by-trace. If the shot statics functions are used, then filter application is by correlation; if inverse filters, then convolution. It is particularly useful to use the trace display to look at each constant-angle gather to judge the effectiveness of the filter application.

FIG. 11. This flow applies the inverse filters derived from the conditioned cross-correlations to the traces of the common-angle gathers, which applies the near-surface corrections.

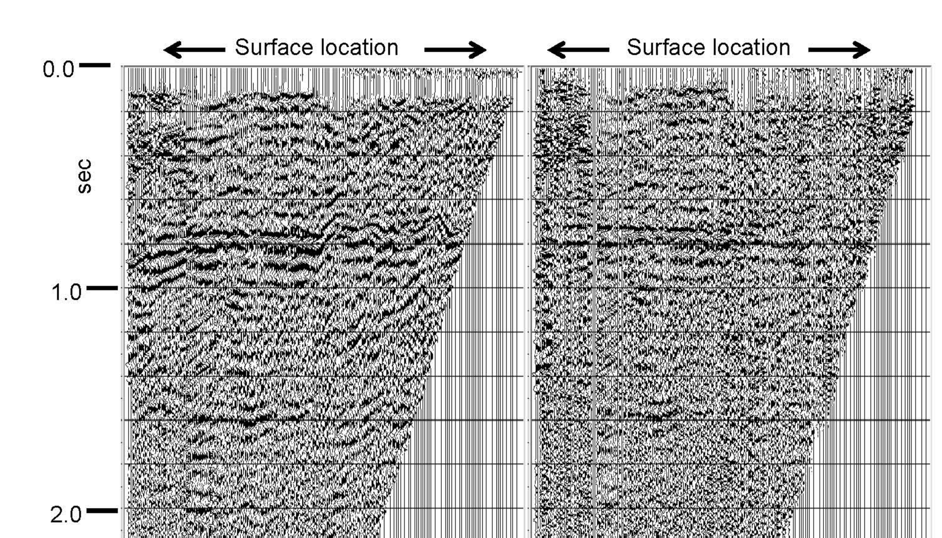

Typical common angle gather before and after interferometric correction

FIG. 12. An example of a common-angle gather (from Spring Coulee) before (left) and after (right) application of the inverse filters (Figure 11)

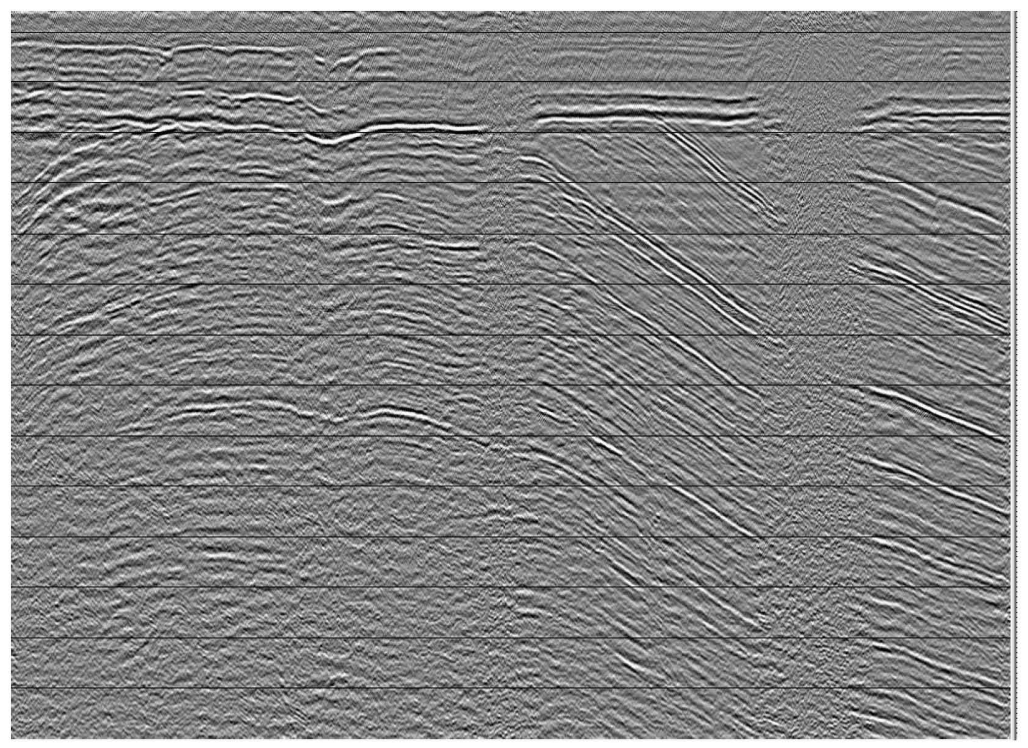

FIG. 13. The brute stack of the MacKenzie Delta line

BEFORE AND AFTER

Figures 13 and 14 show the improvement sometimes possible with raypath interferometry, as the seismic image is improved throughout.

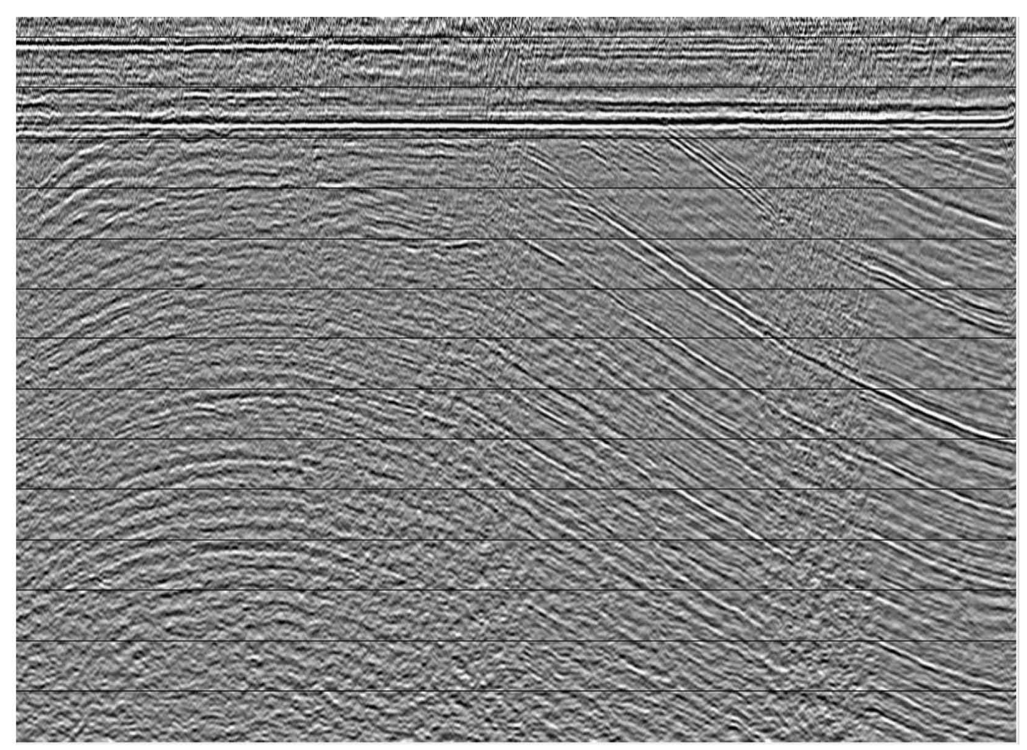

FIG. 14. The MacKenzie Delta line after Raypath interferometry using the two horizons shown in Figure 5.

ACKNOWLEDGEMENTS

Thanks to Shell Canada for the continuing use of the MacKenzie Delta data, and to CREWES sponsors and staff for support.